Environmental Science
Processes & Impacts

Accepted Manuscript

ROYAL SOCIETY OF CHEMISTRY

rsc.li/process-impacts

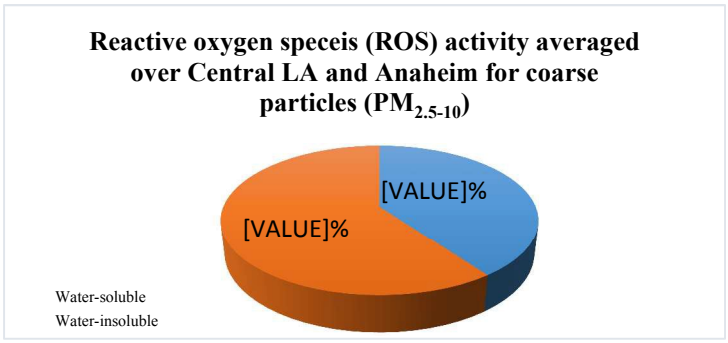

Water-insoluble components constituted a larger fraction of CPM ROS activity. Elemental composition of CPM was highly associated with ROS activity.

Results from this study emphasize the role of non-exhaust traffic emissions, which are currently understudied and largely unregulated, in the potential toxicity of ambient coarse particles. The relative importance of non-exhaust traffic-related emissions has increased as the contribution of vehicle tailpipe emissions to total ambient PM concentrations has decreased due to the stringent regulations in the LA Basin. This manuscript focuses on the ROS activity of the coarse particles with respect to its water solubility and relation to certain metals and trace elements. Two major sources identified by principal component analysis along with their tracers were found to mainly derive the overall toxicity of ambient coarse particles in the LA Basin: abrasive vehicular emissions and re-suspended soil and road dust.

Oxidative potential of coarse particulate matter ($PM_{10-2.5}$) and its relation to water solubility and sources of trace elements and metals in the Los Angeles Basin

Farimah Shirmohammadi[1], Sina Hasheminassab[1], Dongbin Wang[1], Arian Saffari[1], James J. Schauer[2], Martin M. Shafer[2], Ralph J. Delfino[3], Constantinos Sioutas[1*]

[1] University of Southern California, Department of Civil and Environmental Engineering, Los Angeles, CA, USA

[2] University of Wisconsin-Madison, Environmental Chemistry and Technology Program, Madison, WI, USA

[3]University of California, Irvine, Department of Epidemiology, School of Medicine, Irvine, CA, USA

[*]Corresponding author: sioutas@usc.edu

Abstract

In this study, potential sources of water-soluble (WS) and water-insoluble (WI) fractions of metals and trace elements in coarse particulate matter (CPM) ($PM_{10-2.5}$, 2.5<dp<10 μm) were identified and their association with the redox properties of CPM, measured by means of reactive oxygen species (ROS), was explored. CPM was collected during 2012-2013 in Central Los Angeles (LA) and 2013-2014 in Anaheim, CA. Generally, WI components contributed to a larger fraction of CPM ROS activity (as much as 64% and 54% at Central LA and Anaheim, respectively). Two major source factors were identified by Principal Component Analysis for both the WS and WI fractions: vehicular abrasion and re-suspended road dust. Univariate analysis indicated that several species were correlated with CPM ROS activity: In WS fraction, metals such as Mn, Fe, Cd and Zn were associated with WS ROS, while in WI fraction Ti, Fe, Ni, Pb and Cr had the highest correlations with WI ROS activity. Multiple linear regression analysis revealed that both vehicular abrasion and re-suspension of road dust were associated with WS ROS activity, while only vehicular abrasion contributed significantly to the WI ROS activity. Moreover, comparison with previous studies indicated that the ROS activity of CPM has increased in the past 5 years in Central LA. We attribute this increase mainly to the elevated levels of re-suspension of road dust caused by the increase in vehicle speed and number of trucks in recent years in this area, reaffirming the growing importance of non-tailpipe traffic emissions on CPM toxicity.

1. Introduction

Epidemiological and toxicological studies have linked the exposure to particulate matter (PM) in different size ranges , including coarse PM, to adverse health outcomes ranging from cardiovascular and respiratory diseases to neurological disorders [1–8]. There is growing evidence that these adverse health effects are primarily associated with certain PM chemical species, among which metals and trace elements have been demonstrated to be detrimental due to their redox active capability that can contribute to PM toxicity [9–13]. In contrast to organic species and secondary ions which are more abundant in the fine size range ($PM_{2.5}$, dp<2.5 μm), metals and trace elements are more dominant in the coarse size fraction (i.e. $PM_{10-2.5}$, 2.5<dp<10 μm) [14,15].

Road traffic is one of the primary sources contributing to total PM mass concentrations in urban areas [16,17]. Traffic-generated emissions arise from exhaust and non-exhaust sources. Over the past decades, policy and regulations have focused almost exclusively on exhaust emissions, resulting in a significant reduction in the contribution of vehicle tailpipe emissions to total ambient PM concentrations in the LA Basin [17–21]As a consequence of progressive reductions in exhaust emissions, the relative importance of non-exhaust traffic-related emissions has increased: e.g. several studies have shown that the contribution of exhaust and non-exhaust emissions to PM_{10} mass concentrations is almost equal in roadside air [22,23].

Emissions from traffic-related sources are characterized by carbonaceous particles, largely originating from tailpipe emissions, in addition to metals and crustal elements primarily sourced from brake wear and re-suspension of road dust [24]. Unlike $PM_{2.5}$, the production of which is dominated by combustion processes (i.e. exhaust emissions), coarse

particulate matter (CPM) is also a product of non-exhaust emissions such as re-suspension of road dust from the wake of passing traffic, windblown soil, as well as abrasion of road surface, tires and brake wear [16,17]. Studies have been conducted to characterize the metal content of brake linings and brake wear particles [25,26]; and several important tracer elements, such as Fe, Cu, Ba, Pb and Zn, have been observed in particles related to brake linings [17,27–29]. Other elements such as Cd, Cu and Pb are also utilized in tire manufacturing and thus may be emitted from tire-pavement abrasive emissions [17,30]. Another major source of Pb is lead weights used in balancing vehicles wheels which can be eventually grinded in the roadways [31]. Therefore, evaluating the associations between these important metals and PM-induced toxicity remains an important and active topic of aerosol research, despite the recent reductions in vehicular tailpipe emissions. Several studies have suggested that the soluble fraction of metals and trace elements in the atmosphere also plays an important role in PM-induced toxicological responses [32–35].

The generation of reactive oxygen species (ROS) has been postulated to be an important mechanism leading to PM-induced toxicity and associated adverse health effects [36–38]. In this study, the ROS activity of the PM samples was quantified in an in-vitro alveolar macrophage-based assay (NR8383 cell line, ATCC) [39], using the broadly responsive (sensitive to the ROS species, hydroxyl radical, peroxide, superoxide and peroxynitrite) fluorescent probe by de-acetylation of 2′,7′-dichlorofluorescein diacetate (DCFH-DA) [39]. Several studies have documented that the ROS activity measured by this assay in ambient PM is highly correlated with transition metals such as Cu, Fe, V, Ni and Cr [40–44].

The current study focuses on the ROS activity of coarse particulate matter collected at two different locations in the LA Basin (i.e. Central Los Angeles and Anaheim), as part of

the Cardiovascular Health and Air Pollution Study (CHAPS). The goals of the study were to determine the temporal variations of ROS activity in both sampling sites and more importantly, to identify the elements that drive the ROS activity with respect to water-soluble (WS) and water-insoluble (WI) fractions of the PM. Principal component analysis (PCA) was conducted on each fraction to investigate and compare the emission sources of WS and WI metals. Univariate and multiple linear regression analyses were also applied to explore the association of WS and WI metals with the respective fractions of the ROS activity. The ROS levels measured in this study at Central LA were also compared with previous studies conducted at the same sampling location.

2. Experimental

2.1 Sampling sites and meteorology

Ambient CPM samples were collected at two locations in the LA Basin. One site representing an urban area ("Central LA") was located at the Particle Instrumentation Unit at the University of Southern California (USC), positioned within 150 m downwind of a major freeway (I-110). The other site was located about 40 km southeast of downtown LA in Anaheim and is representative of a suburban/residential area. Selected meteorological parameters at these sites including monthly-averaged temperature, relative humidity, wind speed and wind direction were acquired from the South Coast Air Quality Management District (SCAQMD) online database and are presented in a companion paper (Shirmohammadi et al., 2015). Throughout this manuscript, "warmer months" refers to the July to September period, while "colder months" refers to October to February. Briefly, average temperature varied from 22.2 ± 2.02 ºC in warmer months to 15.1 ± 3.14 ºC in

colder months at Central LA, whereas it spanned a range of 22.2 ± 0.47 to 16.3 ± 1.65 ºC in Anaheim. During the warmer months, average relative humidity was 65.6 ± 3.70% and 62.2 ± 2.33% at Central LA and Anaheim, respectively, while these values were reduced to 59.6 ± 9.69% and 55.3 ± 7.69% in colder months. Wind speed at Central LA varied from an average of 10 ± 3.3 kph in warmer months to 4.5 ± 1.5 kph in colder months. Anaheim had lower average wind speeds in comparison to Central LA ranging from the mean value of 3.4 ± 0.6 to 1.6 ± 0.9 kph from warmer months to colder months, respectively.

2.2 Sampling schedule and method

Time-integrated sampling was conducted over five contiguous days (Monday to Friday) each week between July 2012 and February 2013 at Central LA, and from Sunday to Thursday, each week between July 2013 and February 2014 in Anaheim except for December 2013. Sampling in Anaheim was discontinued in December 2013 and resumed in January 2014. At each sampling site, ambient particles were collected within three size ranges (<0.18 μm (ultrafine), 0.18-2.5 μm (accumulation), and 2.5-10 μm (coarse)) using two parallel sampling Micro-Orifice Uniform Deposit Impactors (MOUDIs, Model 110, MSP Corporation), with a flow rate of 30 L/min. Although the flow rate was set at 30 L/min, in a few cases (by no more than 5-7%), the flow rate was measured lower than 30 L/min at the end of sampling, mainly due to the increased pressure drop caused by relatively high concentrations of ambient PM. One MOUDI was loaded with 47-mm Teflon filters (Teflo, Pall Life Sciences, 1-μm pore, Ann Arbor, MI), while the other sampler was loaded with pre-baked aluminum-foil substrates in the coarse and accumulation stages and quartz microfiber filters (Whatman International Ltd, Maidstone,

England) in the ultrafine stage. This study presented here focuses entirely on the coarse mode.

2.3 Gravimetric and chemical analysis

Gravimetric mass (PM mass concentration) was determined from the Teflon filters. The substrates were stabilized under controlled temperature (22–24 °C) and relative humidity (40-50%) and weighed before and after the sampling using a microbalance (± 0.001 mg) (Mettler Toledo Inc., Columbus, OH, USA). Total elemental composition of the CPM samples was measured by digestion of a section of the filter-collected PM using a microwave aided, sealed bomb, mixed acid digestion (HNO_3, HF and HCL). Digests were subsequently analyzed by high resolution inductively coupled plasma sector field mass spectrometry (SF-ICPMS). The water-soluble fraction of the elements was also determined by SF-ICPMS after water extraction (10 ml Milli-Q water (Millipore, Bedford, MA, USA), 0.22 μm filtration) of a separate section of the filters.

Macrophage reactive oxygen species (ROS) production was quantified by first extracting another section of the filter with 1.00 ml of Milli-Q water with continuous agitation for 16 h at room temperature and then exposing (in 96-well plates) rat alveolar macrophage cells (NR8383, American Type Culture Collection) to both unfiltered and filtered (0.22 μm polypropylene syringe filters) PM extracts. Prior to sample exposure, the macrophage cells are loaded with the fluorescent probe DCFH-DA (2′,7′-dichlorofluorescein diacetate). DCFH-DA is membrane permeable and in the cytoplasm of the cell is deacetylated by cellular esterases to DCHF (2′,7′-dichlorodihydrofluorescein). DCFH is oxidized by ROS to 2,7-dichlorofluorescein (DCH) which is highly fluorescent and can be detected by a

micro-plate reader. ROS activity was normalized and reported in units of Zymosan equivalents [45]. The ROS activity assay was performed on both filtered and unfiltered PM extracts. As in the WS ROS, filtered extracts for ROS measurement were prepared by processing the bulk extract (suspension of particles and soluble species) through a 0.22 μm syringe filter and collecting the filtrate (filter-passing). For Total ROS, subsamples of the bulk extract are analyzed without filtration. The extraction protocol for the ROS measurement has been shown to recover about 80 to 105 percent of the mass loaded on the filter [46]. The WI ROS fraction was then calculated as the difference between Total and WS ROS activity.

2.4 Statistical analysis

2.4.1 Principal component analysis (PCA)

Principal component analysis was applied to the two extract fractions (WS and WI elements) separately, each comprising the combined dataset of weekly samples from both Central LA and Anaheim. PCA analysis is a variable reduction procedure, which seeks to explain most of the variance in a set of observed variables by relatively small number of components. A VARIMAX-normalized rotation was applied to determine uncorrelated components [47] and those with eigenvalues above unity were included as potential source factors. Data from both sites were pooled together primarily to increase the statistical power of the analysis. Elements were then attributed to a certain source factor when they showed loadings above 0.7 in a given component. As a result, source identification was based on the presence of certain metals and elements in a given component.

2.4.2 Multiple linear regression (MLR)

Multiple linear regression was applied to the combined dataset of weekly concentration of WS and WI elements and ROS, separately in order to identify the species (independent variables) which contribute to ROS activity (dependent variable) mostly. To this end, MLR analysis was applied with various combinations of species especially those which showed high correlations with ROS activity. A set of species which were significant ($p < 0.05$) and not co-linear with each other were kept while trying to reach the highest R^2 value to predict ROS activity to a reasonable extent.

3. Results and discussion

3.1 Temporal variations in CPM mass concentrations in the sampling sites

In current study, the CPM mass concentrations averaged 22.6±3.5 μg/m^3 in the warmer months to 11.5±3.3 μg/m^3 in the colder months at Central LA. The seasonal variation was much more limited at Anaheim (13.5±2.2 in summer to 10.0±2.3 μg/m^3 in winter). Higher CPM mass concentrations at Central LA are mainly attributed to the proximity of the sampling site to a major freeway (I-110) and higher regional density of traffic along with higher levels of wind speed at this site in comparison to Anaheim, leading to enhanced re-suspension of soil and road dust at this site. Figure 1 (a-b) presents the monthly-averaged CPM mass concentration at Central LA and Anaheim.

In Central LA, Pakbin et al. [28] reported an average CPM mass concentration of 11.6±3.5 μg/m^3 from July 2008 to February 2009, during the corresponding sampling months in this study, indicating that over 4 years, CPM concentrations have increased by approximately

35% in Central LA. Moreover, CPM mass concentration in this study was higher by almost 25% in comparison with the levels reported by Cheung et al. [40] at Central LA and in the corresponding sampling months. This increasing trend in the levels of CPM mass concentration is in line with the findings of Cheung et al.[48], who showed a continual, yet moderate increase in the levels of CPM mass concentrations after 2005 in Central LA and future studies will further validate this trend.

3.2 Temporal variations in ROS activity

The monthly-averaged ROS activity of coarse particles, in both WS and WI fractions, normalized by the volume of air (i.e. expressed in μg Zymosan per m^3 of air) at the two sampling sites is shown in Figure 2 (a-b). In comparison with PM mass normalized ROS activity (in μg Zymosan/mg PM), the volume-based ROS activity is a more relevant metric for comparison of inhalation exposures. On a per volume basis, ROS was generally higher in warmer months than colder months with averages of 119 ± 32.1 and 65.0 ± 26.5 μg Zymosan/m^3 air in Central LA, respectively. The relatively higher per volume ROS activity in the warmer season is mainly attributed to higher CPM mass concentration levels during this period of time, as a result of higher wind speed and lower relative humidity, as discussed in previous sections. Coarse PM at Anaheim, on the other hand, displayed lower ROS activity levels in comparison to Central LA, with average values spanning a very narrow range from 21.4 ± 4.1 μg Zymosan/m^3 air in warmer months to 23.1 ± 2.0 μg Zymosan/m^3 air in colder months. This narrow range is consistent with the small variation in CPM mass concentrations measured at this site, but also with the possibility of less temporally variable sources of CPM at this site. As it will be discussed in following

sections, the higher ROS level at Central LA is mainly attributed to more pronounced contributions by traffic-related emissions due to proximity of this site to major roadways, and therefore, higher levels of redox active species such as transition metals.

The monthly-averaged ROS activity of coarse particles expressed in μg Zymosan per mg of PM units, is presented in Figure 3 (a-b) for Central LA and Anaheim. Averaged across all sampling months, ROS values showed higher levels at Central LA compared to Anaheim ($5.29\times10^{3}\pm1.09\times10^{3}$ and $2.08\times10^{3}\pm0.603\times10^{3}$ μg Zymosan/mg PM, respectively). Higher per mass ROS activity at Central LA again underscores the potential impact of traffic-related emissions and associated trace elements on PM toxicity in this size range.

As evident from Figures 2 and 3, a substantial fraction of CPM ROS activity is attributed to the WI portion (64 and 54 % of total volume-based ROS at Central LA and Anaheim, respectively, on average, over all sampling months), indicating that WI components in the coarse size fraction, such as important WI metals (i.e. Fe, Cr, Ni, Pb) play a significant role in the overall CPM toxicity. A detailed discussion on the association of the WS and WI metals on the respective fractions of ROS is provided in the following sections.

3.3 Concentration of WS and WI elements

Figure 4 (a-b) displays the geometric mean concentrations of WS and WI metals at Central LA and Anaheim, over all sampling months. In the WS fraction, most species concentrations spanned a range of 0.001-1 ng/m^3 with higher levels observed at Central LA in comparison to Anaheim. It is evident that most elements had higher concentrations

in the WI than WS fraction, indicating relatively low solubility across all of these species. As can be seen from Figures 4 (a-b), most elements, including the metals Cd, Cr, Cu, Fe, Ni, Pb and V had higher concentrations at Central LA than Anaheim, likely due to the greater proximity of this site to roadways in addition to higher regional density of traffic compared to Anaheim. Higher concentration of these species at Central LA may in-part explain the higher ROS activity observed at this site, since, as will be demonstrated in the following sections, these metals exhibit strong correlations with ROS activity. The temporal variations in selected metal concentrations for the WS and WI fractions at the two sampling sites are presented in Figures 5 and 6, respectively. Overall, at Central LA WS metals concentration peak in warmer months. In the WI fraction, the majority of metals, except for Fe, showed higher concentrations during the colder months. In Anaheim, both WS and WI have generally higher concentrations during colder months, except for Cr, Ni and V in WI fraction. These findings may explain the higher ROS activity at Central LA in addition to the higher contribution from WI fraction of ROS activity to total per volume ROS activity. Table S1 presents the water solubility fraction of selected species at Central LA and Anaheim, indicating the overall higher concentrations of the WI fraction of the aforementioned species at both sampling sites. Comparison of the same set of metals (expressed as ng/μg PM) at Central LA and Anaheim is also presented in Figure S1.

3.4 Sources of WS and WI metals and associations with the ROS activity

3.4.1 Source factors of WS and WI metals

To investigate the potential sources of WS and WI metals in the CPM, a PCA was applied to datasets comprising the pooled data from both Central LA and Anaheim. The

PCA results of site-combined datasets for the WS and WI elements are presented in Table 1 (a-b). Several studies have applied factor analysis on a number of sites pooled together [49–51]. Mooibroek et al [52] who carried out a positive matrix factorization (PMF) model on a combined dataset from 5 distinct sites in the Netherlands argue that by combining the datasets, PCA provides insight on sources affecting all receptor sites, and therefore focuses on PM formation processes dominant across sites, while downplaying the effects of unique local variations.

Two major principal components were identified for both the WS and WI fractions. In the WS fraction the first principal component likely represents vehicular abrasion from tire and brake wear, with strong contributions from Ba, Sb, Mo, Rh, Cu, Mn and Zn. These elements are among the more water-soluble species. This component accounted for 46.2% of the total variance. Previous studies [28,53,54] have also reported high loadings of Ba, Sb, Mo, and Cu, as well as Rh, Fe and Pb in abrasive vehicular emissions. Several studies have reported the elemental composition of brake dust PM. Thorpe and Harrison [17] reported Cu, Ba and Sb as the most common brake dust tracers. Cu is used as a high-temperature lubricant, while $BaSO_4$ is used as a filler in brake lining formulation, and Sb_2S_3 is used as an alternative to asbestos in brake linings [17,55]. The second principal component had high factor loadings of Na, Mg, S, Fe and Ca; therefore, this component was attributed to the re-suspension of soil and road dust. This component constituted 45.2% of total variance for water-soluble fraction. Lough et al. [56] have also reported Na, Mg, Ca and Fe as typical tracers of re-suspended road dust in a tunnel study in Milwaukee. Moreover, in another study carried out in Beijing Han et al. [57] reported high concentration of Ca and S in re-suspended road dust.

For the WI fraction, two principal components were also identified, with very similar profiles to those resolved for the WS fraction. In the first principal component, high loadings of Al, Nd, Rb, Pr, Ti, Y, Mn, and Pb, likely representing water insoluble components of re-suspended soil and road dust, were observed. Previous studies have also identified road dust as a major source of coarse particle emissions in different locations around the world [28,58]. Al, Mn, and Ti were observed in tire wear emissions together with road dust, in a study Wåhlin et al. [54] conducted in Copenhagen, Denmark. Furthermore, Pakbin et al. [28] have also attributed Al, Nd, Rb, Pr, Ti, Y and Mn to re-suspension of soil and road dust in the Los Angeles area. Lead has been prohibited for several decades as an additive to gasoline fuels thus direct tailpipe emissions are minimal; however, Pb is commonly used in wheel balancing weights and this along with other sources result in high emissions in road dust environments [17,31]. The second principal component appears to be indicative of vehicular abrasion, with high loadings of Sb, Mo, Cu, Cr, Fe and Ni. As mentioned previously, Sb, Mo, Fe and Cu have also been reported by Pakbin et al. [28] as tracers of abrasive vehicular emissions in the LA area, and Ni and Cr have been also identified in brake linings of passenger cars by Westerlund et al. [59]. In this study, re-suspended soil and road dust and vehicular abrasion accounted for 54.2% and 32.3% of total variance for WI metals, respectively.

Overall, similar source factors have been identified by PCA for WS and WI metals, in which re-suspension of soil and road dust, as well as vehicular abrasion were the two dominant source factors. Using almost two independent and chemically different sets of marker species, the similar source profiles identified by PCA illustrate that overall the same sources contribute to WS and WI metals in the coarse PM size fraction. This is

consistent with the study by Pakbin et al. [28] who also reported that road dust and vehicular abrasion were the two dominant sources of total CPM metals over 10 sampling sites in the LA Basin.

3.4.2 Univariate analysis

Univariate analysis was carried out in order to investigate the association of ROS activity with specific elements in both WS and WI fraction of the CPM. Table 2 (a-b) presents the Pearson correlation coefficients (R) between weekly volume-based ROS activity data and WS and WI metals concentrations. The species exhibiting strong correlation and statistically significant (defined here as associations with $R > 0.70$ and $p < 0.05$) with the ROS activity are highlighted in bold in the Table 2. As can be seen in Table 2a, the majority of WS metals such as Cu, Fe, Ca, Mn, As and Cd have strong correlations with WS ROS activity and are mainly associated with re-suspension of road dust or vehicular abrasions. These results are consistent with the findings of several previous studies [40,43,60]. For WI metals Ni, Cr and Fe displayed higher correlations with WI ROS activity. Previous studies have also documented the associations between water-insoluble fraction of these metals and ROS activity in the coarse size fractions [32,44,61]. The temporal variability (Figures 5 and 6) of a number of these elements in both sampling sites illustrate the covariance with ROS activity discussed in previous sections.

3.4.3 Multiple linear regression analysis

The univariate analysis in the previous section revealed information about the individual association of metals and ROS activity, and also provided insight into which metals should be considered for inclusion in a multivariate regression analysis to determine the relative importance of these metals to the ROS activity. The following equations were obtained for the prediction of WS and WI ROS activity using WS and WI metals. The species included in the model are all statistically significant ($p < 0.05$) and present the best linear fit, and thus are considered as the potential predictors of ROS activity:

$$\text{WS ROS} = 4.13 + 0.912 * \text{WS Cu} + 4.34 * \text{WS Fe} \quad [1]$$

$$\text{WI ROS} = -16.09 + 22.23 * \text{WI Cr} + 80.08 * \text{WI Ni} \quad [2]$$

where the ROS activity and metals concentrations are expressed in μg Zymosan/m^3 air and ng/m^3, respectively. The modeled ROS based on the above equations are also plotted against measured ROS in Figure 7 (a-b). The appearance of Cu and Fe in the first equation underscores the strong impact of both vehicular abrasion and re-suspended road dust on ROS activity. Cu and Fe can explain a large fraction of the variance in WS ROS activity, as shown in Figure 7a (R^2= 0.89, slope=0.99 and intercept= 0.45 μg Zymosan/m^3 air). Cr and Ni, which are both representative of vehicular abrasion in our PCA model, can also explain 64% of the total variance in WI ROS, as indicated in Figure 7b (R^2= 0.64, slope=1.01 and intercept= -0.04 μg Zymosan/m^3 air). Therefore, it can be concluded that the majority of the ROS activity in CPM can be attributed to two major factors (sources): re-suspended road dust and vehicular abrasion. These findings altogether underscore the

fact that non-exhaust emissions can have a very significant role in the toxicity levels observed in coarse PM size range.

3.5 Comparison with previous studies

In order to investigate the trends in elemental concentrations as well as ROS activity over the past few years in the LA region, the results of the current study was compared to those in a study by Cheung et al. [40], which was conducted in July-August 2009 and January-February 2010 across four distinct time periods with daily sampling in Central LA at the same sampling site. To align our comparison, the data of the Cheung et al. [40] study were averaged into monthly periods corresponding to the same sampling months of our study. Moreover, Hasheminassab et al. [19] have shown that the meteorological conditions in terms of temperature, relative humidity and precipitation were consistent during the 2002 to 2013 period in the LA Basin, and the averaged wind speeds during the corresponding months between 2009-2010 and 2012-2013 were also comparable. Figures 8 and 9 present the volume-based ROS activity and groups of metals and elements compared with Cheung et al. [40] at Central LA. The ROS activity reported by Cheung et al. [40] was determined by filtered extraction of aqueous suspensions of PM through a 0.22 μm syringe filter, and therefore corresponds to the WS fraction of ROS activity in the present study. The average WS ROS level in the present study was 28.2±25.6 μg Zymosan/m^3 air, which is about 2.8 times higher (Mann- Whitney Rank Sum Test, $p < 0.01$) than the value reported by Cheung et al. [40]. This quite substantial difference could be mainly attributed to the increase in levels of metals and trace elements in this size range over the years in Central LA. As illustrated in the box plots of Figure 9, comparison of median values of the three groups of

metals revealed an overall increase from the 2009-2010 period to the 2012-2013 period: vehicular abrasion tracers, which represent the sum of Ba, Sb, Mo, Fe, Cu, Mn, Cr, Ni, As, Pb, Sr and Zn [17,28,53,54,59], has increased by about 50%, although this increase was not found to be statistically significant ($p = 0.4$). The road dust group (sum of Al, Rb, Ti, Fe, Mn, Ca and Nd) also increased significantly ($p < 0.01$) by almost 2 –fold. Other metals and elements (i.e., the sum of Na, S, K, Mg, Pb, V, As, La, Co, Y and Cd) increased by a factor of about 4.4 ($p < 0.001$). Comparisons based on mass-based ROS and metal levels are also presented in Figures S2 and S3, which reveal similar trends between these two studies to those observed for the per m^3 air volume data.

Harrison et al. [22] demonstrated that the turbulence caused by passing vehicles at two urban sites in London acts as a strong source of re-suspended soil and road dust, to such an extent that the source strength is comparable to that of vehicular exhaust emissions for fine particles. The authors postulated that the majority of coarse particles originate from re-suspension of soil and road dust from the turbulence caused by the passing traffic. In Central LA, Cheung et al. [40] have also observed high contribution of the re-suspension mechanism to CPM total mass and metals concentrations, induced by higher speed of passing vehicles and larger fractions of heavy-duty trucks during nighttime in winter. To explore the causes of the considerable increase in trace elements and metals, particularly those from re-suspended soil and road dust in this study compared to those reported by Cheung et al. [40] we conducted the following analysis; the daily-averaged number of trucks and speed of vehicles passing by the nearest vehicle detection station closest to our sampling site in Central LA were obtained from the freeway performance measurement system (PeMS) for the two study periods. Figure S4 (a-b) show the box plots of the daily-

averaged speed of vehicles (as a metric of turbulence in freeways) and number of trucks in 2009-2010 (corresponding to Cheung et al.'s [40] sampling year) and 2012-2013 (corresponding to the current study). The median values of vehicle's speed and number of trucks increased by 6% and 15%, respectively, from 2009-2010 to 2012-2013. Mann-Whitney Rank Sum Test also indicated that these increases were statistically significant ($p < 0.001$). This elevation is in line with the observed trend in the number of trucks reported by Regional Transportation Plan (RTP) in Southern California (Federal Highway Administration's Office of Freight Management). These trends over the past 3 years altogether support the measured overall increase in the levels of tracers of vehicular abrasion mixed with crustal materials and trace elements documented in the current study. An additional factor contributing to the increase in metals and trace elements concentrations could be the state of California drought of the past 3 years, resulting in restricted water use and affecting street cleanings, which could lead to enhanced re-suspended soil and road dust.

4. Conclusions

To determine the elemental composition of coarse particles and its association with ROS activity, time-integrated sampling was conducted at Central LA from July 2012 to February 2013 and at Anaheim from July 2013 to February 2014. Overall, higher ROS activity levels were observed at Central LA compared to Anaheim, which is most likely contributed by higher levels of some important redox active species at Central LA. The water-insoluble ROS fraction constitutes 64% and 54% of total ROS at Central LA and Anaheim, respectively. PCA analysis revealed two major sources of metals (i.e. re-

suspension of soil/road dust and vehicular abrasion) for both water-soluble and insoluble fractions. Univariate and multivariate regression analysis showed some important species (i.e. Fe, Cu, Cr and Ni) were highly correlated with the water-soluble and insoluble ROS activity. Results from this study also suggest that the potential sources of CPM metals are relatively similar in water-soluble and insoluble fractions, where re-suspension of road dust and vehicular abrasion emissions play a significant role in ROS activity. Comparison to a previous study conducted at Central LA by Cheung et al. [40] revealed that ROS activity level has increased over the years, which is most likely due to the increase in vehicle speed and number of trucks over the years in Los Angeles, again underscoring the importance of re-suspension of road dust and vehicular abrasion as major sources contributing to CPM toxicity. Moreover, recent state of California drought and consequently restricted water use could affect street cleanings and therefore be another potential reason for elevated levels of re-suspended soil and road dust. Results from this study emphasize the role of non-exhaust traffic emission, which are currently understudied and largely unregulated on the toxicity of coarse PM.

5. Acknowledgements

The present project was supported by grant numbers ES12243 from the National Institute of Environmental Health Sciences, U.S. National Institutes of Health. The authors wish to thank the staffers at the Wisconsin state laboratory of hygiene for their assistance with the chemical analysis. We also acknowledge the support of USC's Provost and Viterbi PhD fellowships.

6. References

1 B. Brunekreef and B. Forsberg, *Eur. Respir. J.*, 2005, **26**, 309–318.

2 A. Campbell, M. Oldham, A. Becaria, S. C. Bondy, D. Meacher, C. Sioutas, C. Misra, L. B. Mendez and M. Kleinman, *NeuroToxicology*, 2005, **26**, 133–140.

3 R. J. Delfino, N. Staimer, T. Tjoa, M. Arhami, A. Polidori, D. L. Gillen, M. T. Kleinman, J. J. Schauer and C. Sioutas, *Environ. Health Perspect.*, 2010, **118**, 756–762.

4 W. J. Gauderman, R. Urman, E. Avol, K. Berhane, R. McConnell, E. Rappaport, R. Chang, F. Lurmann and F. Gilliland, *N. Engl. J. Med.*, 2015, **372**, 905–913.

5 C. A. Pope III and D. W. Dockery, *J. Air Waste Manag. Assoc.*, 2006, **56**, 709–742.

6 B. J. Malig, S. Green, R. Basu and R. Broadwin, *Am. J. Epidemiol.*, 2013, **178**, 58–69.

7 M. Morishita, R. L. Bard, L. Wang, R. Das, J. T. Dvonch, C. Spino, B. Mukherjee, Q. Sun, J. R. Harkema, S. Rajagopalan and R. D. Brook, *J. Expo. Sci. Environ. Epidemiol.*, 2015, **25**, 153–159.

8 A. Zanobetti and J. Schwartz, *Environ. Health Perspect.*, 2009, **117**, 898–903.

9 R. S. Chapman, W. P. Watkinson, K. L. Dreher and D. L. Costa, *Environ. Toxicol. Pharmacol.*, 1997, **4**, 331–338.

10 J. G. Charrier and C. Anastasio, *Atmospheric Chem. Phys. Print*, 2012, **12**, 11317–11350.

11 R. M. Harrison and J. Yin, *Sci. Total Environ.*, 2000, **249**, 85–101.

12 J. S. Lighty, J. M. Veranth and A. F. Sarofim, *J. Air Waste Manag. Assoc.*, 2000, **50**, 1565–1618.

13 T. Shi, R. P. F. Schins, A. M. Knaapen, T. Kuhlbusch, M. Pitz, J. Heinrich and P. J. A. Borm, *J. Environ. Monit.*, 2003, **5**, 550–556.

14 K. Cheung, N. Daher, W. Kam, M. M. Shafer, Z. Ning, J. J. Schauer and C. Sioutas, *Atmos. Environ.*, 2011, **45**, 2651–2662.

15 C. Hueglin, R. Gehrig, U. Baltensperger, M. Gysel, C. Monn and H. Vonmont, *Atmos. Environ.*, 2005, **39**, 637–651.

16 P. Pant and R. M. Harrison, *Atmos. Environ.*, 2013, **77**, 78–97.

17 A. Thorpe and R. M. Harrison, *Sci. Total Environ.*, 2008, **400**, 270–282.

18 G. A. Bishop, B. G. Schuchmann and D. H. Stedman, *Environ. Sci. Technol.*, 2013, **47**, 9523–9529.

19 S. Hasheminassab, N. Daher, B. D. Ostro and C. Sioutas, *Environ. Pollut.*, 2014, **193**, 54–64.

20 M. Mathissen, V. Scheer, R. Vogt and T. Benter, *Atmos. Environ.*, 2011, **45**, 6172–6179.

21 B. C. McDonald, A. H. Goldstein and R. A. Harley, *Environ. Sci. Technol.*, 2015, **49**, 5178–5188.

22 R. M. Harrison, J. Yin, D. Mark, J. Stedman, R. S. Appleby, J. Booker and S. Moorcroft, *Atmos. Environ.*, 2001, **35**, 3667–3679.

23 X. Querol, A. Alastuey, M. M. Viana, S. Rodriguez, B. Artiñano, P. Salvador, S. Garcia do Santos, R. Fernandez Patier, C. R. Ruiz, J. de la Rosa, A. Sanchez de la Campa, M. Menendez and J. I. Gil, *J. Aerosol Sci.*, 2004, **35**, 1151–1172.

24 E. Furusjö, J. Sternbeck and A. P. Cousins, *Sci. Total Environ.*, 2007, **387**, 206–219.

25 D. Chan and G. W. Stachowiak, *Proc. Inst. Mech. Eng. Part J. Automob. Eng.*, 2004, **218**, 953–966.

26 J. J. Schauer, G. C. Lough, M. M. Shafer, W. F. Christensen, M. F. Arndt, J. T. DeMinter and J. S. Park, *Res. Rep. Health Eff. Inst.*, 2006, 1–76; discussion 77–88.

27 F. Amato, M. Pandolfi, T. Moreno, M. Furger, J. Pey, A. Alastuey, N. Bukowiecki, A. S. H. Prevot, U. Baltensperger and X. Querol, *Atmos. Environ.*, 2011, **45**, 6777–6787.

28 P. Pakbin, Z. Ning, M. M. Shafer, J. J. Schauer and C. Sioutas, *Aerosol Sci. Technol.*, 2011, **45**, 949–963.

29 F. Song and Y. Gao, *Atmos. Environ.*, 2011, **45**, 6714–6723.

30 M. Legret and C. Pagotto, *Sci. Total Environ.*, 1999, **235**, 143–150.

31 R. A. Root, *Environ. Health Perspect.*, 2000, **108**, 937–940.

32 P. I. Jalava, R. O. Salonen, A. S. Pennanen, M. S. Happo, P. Penttinen, A. I. Hälinen, M. Sillanpää, R. Hillamo and M.-R. Hirvonen, *Toxicol. Appl. Pharmacol.*, 2008, **229**, 146–160.

33 A. M. Knaapen, T. Shi, P. J. A. Borm and R. P. F. Schins, in *Oxygen/Nitrogen Radicals: Cell Injury and Disease*, eds. V. Vallyathan, X. Shi and V. Castranova, Springer US, Boston, MA, 2002, pp. 317–326.

34 M. Sørensen, R. P. F. Schins, O. Hertel and S. Loft, *Cancer Epidemiol. Biomarkers Prev.*, 2005, **14**, 1340–1343.

35 M. Valko, C. J. Rhodes, J. Moncol, M. Izakovic and M. Mazur, *Chem. Biol. Interact.*, 2006, **160**, 1–40.

36 N. Li, C. Sioutas, A. Cho, D. Schmitz, C. Misra, J. Sempf, M. Wang, T. Oberley, J. Froines and A. Nel, *Environ. Health Perspect.*, 2003, **111**, 455–460.

37 A. Nel, *Science*, 2005, **308**, 804–806.

38 F. Tao, B. Gonzalez-Flecha and L. Kobzik, *Free Radic. Biol. Med.*, 2003, **35**, 327–340.

39 A. P. Landreman, M. M. Shafer, J. C. Hemming, M. P. Hannigan and J. J. Schauer, *Aerosol Sci. Technol.*, 2008, **42**, 946–957.

40 K. Cheung, M. M. Shafer, J. J. Schauer and C. Sioutas, *Environ. Sci. Technol.*, 2012, **46**, 3779–3787.

41 M. M. Shafer, D. A. Perkins, D. S. Antkiewicz, E. A. Stone, T. A. Quraishi and J. J. Schauer, *J. Environ. Monit.*, 2010, **12**, 704–715.

42 V. Verma, M. M. Shafer, J. J. Schauer and C. Sioutas, *Atmos. Environ.*, 2010, **44**, 5165–5173.

43 V. Verma, Z. Ning, A. K. Cho, J. J. Schauer, M. M. Shafer and C. Sioutas, *Atmos. Environ.*, 2009, **43**, 6360–6368.

44 D. Wang, P. Pakbin, M. M. Shafer, D. Antkiewicz, J. J. Schauer and C. Sioutas, *Atmos. Environ.*, 2013, **77**, 301–310.

45 A. P. Landreman, M. M. Shafer, J. C. Hemming, M. P. Hannigan and J. J. Schauer, *Aerosol Sci. Technol.*, 2008, **42**, 946–957.

46 A. Saffari, S. Hasheminassab, D. Wang, M. M. Shafer, J. J. Schauer and C. Sioutas, *Atmos. Environ.*, 2015, **120**, 286–296.

47 R. C. Henry, *Atmospheric Environ. 1967*, 1987, **21**, 1815–1820.

48 K. Cheung, M. M. Shafer, J. J. Schauer and C. Sioutas, *J. Air Waste Manag. Assoc.*, 2012, **62**, 541–556.

49 F. Amato and P. K. Hopke, *Atmos. Environ.*, 2012, **46**, 329–337.

50 B. R. Larsen, S. Gilardoni, K. Stenström, J. Niedzialek, J. Jimenez and C. A. Belis, *Atmos. Environ.*, 2012, **50**, 203–213.

51 M. C. Minguillón, X. Querol, U. Baltensperger and A. S. H. Prévôt, *Sci. Total Environ.*, 2012, **427–428**, 191–202.

52 D. Mooibroek, M. Schaap, E. P. Weijers and R. Hoogerbrugge, *Atmos. Environ.*, 2011, **45**, 4180–4191.

53 S. Jj, L. Gc, S. Mm, C. Wf, A. Mf, D. Jt and P. Js, *Res. Rep. Health Eff. Inst.*, 2006, 1–76; discussion 77–88.

54 P. Wåhlin, R. Berkowicz and F. Palmgren, *Atmos. Environ.*, 2006, **40**, 2151–2159.

55 H. Jang and S. J. Kim, *Wear*, 2000, **239**, 229–236.

56 G. C. Lough, J. J. Schauer, J.-S. Park, M. M. Shafer, J. T. DeMinter and J. P. Weinstein, *Environ. Sci. Technol.*, 2005, **39**, 826–836.

57 L. Han, G. Zhuang, S. Cheng, Y. Wang and J. Li, *Atmos. Environ.*, 2007, **41**, 7485–7499.

58 F. Amato, M. Pandolfi, A. Escrig, X. Querol, A. Alastuey, J. Pey, N. Perez and P. K. Hopke, *Atmos. Environ.*, 2009, **43**, 2770–2780.

59 K.-G. Westerlund, *SLB-Anal.*, 2001.

60 A. Saffari, N. Daher, M. M. Shafer, J. J. Schauer and C. Sioutas, *Atmos. Environ.*, 2013, **79**, 566–575.

61 J.-C. Lee, Y.-O. Son, P. Pratheeshkumar and X. Shi, *Free Radic. Biol. Med.*, 2012, **53**, 742–757.

Figures and Tables

Table 1 (a-b). Principal component loadings (VARIMAX normalized) of selected a) water-soluble and b) water-insoluble metals in airborne coarse particulate matter. Loadings higher than 0.7 are shown in bold.

a) Water-soluble

	Principal component	
	Vehicular abrasion	Re-suspended soil/road dust
Ba	**0.97**	0.16
Sb	**0.94**	0.11
Mo	**0.91**	0.31
Rh	**0.87**	0.40
Cu	**0.80**	0.48
Mn	**0.74**	0.63
Zn	**0.73**	0.60
Na	0.18	**0.96**
Mg	0.21	**0.96**
S	0.24	**0.95**
Fe	0.34	**0.88**
Ca	0.59	**0.77**
As	0.59	0.69
Cd	0.62	0.67
Eigenvalue	6.47	6.33
%Variance	46.19	45.23
Cumulative%	46.19	91.42

b) Water-insoluble

	Principal component	
	Re-suspended soil/road dust	Vehicular abrasion
Al	**0.99**	0.02
Nd	**0.97**	0.18
Rb	**0.97**	-0.11
Pr	**0.95**	0.26
Ti	**0.91**	0.38
Y	**0.88**	0.25
Mn	**0.83**	0.36
Pb	**0.70**	0.59
Sb	0.06	**0.97**
Mo	0.13	**0.96**
Cu	-0.14	**0.85**
Cr	0.50	**0.83**
Fe	0.58	**0.80**
Ni	0.45	**0.75**
Eigenvalue	8.13	5.29
%Variance	54.21	35.25
Cumulative%	54.21	89.46

Table 2 (a-b). Pearson correlation coefficients (R) between: a) selected water-soluble metals (ng/m^3) and water-soluble ROS activity (µg Zymosan/m^3 air) and b) selected water-insoluble metals (ng/m^3) and water-insoluble ROS activity (µg Zymosan/m^3 air). Weekly data from both sampling sites were pooled together for this analysis. Values with $R > 0.7$ and $p < 0.05$ are bold.

a)

Metals	*R*
Fe	**0.94**
S	**0.85**
Mn	**0.83**
Ca	**0.82**
Mg	**0.80**
Cu	**0.79**
As	**0.79**
Na	**0.79**
Zn	**0.78**
Cd	**0.75**
Rh	**0.71**
Mo	0.61
Ba	0.54
Sb	0.47

b)

Metals	*R*
Pb	**0.84**
Ni	**0.82**
Nd	**0.74**
Ti	0.65
Cr	0.61
Fe	0.62
Al	0.57
Y	0.51
Mn	0.47
Rb	0.42
Mo	0.32
Sb	0.16
Cu	-0.09
Pr	-0.36

Figure 1 (a-b). Monthly- averaged coarse particles mass concentrations at a) Central LA and b) Anaheim. Error bars are 1 standard deviation. Data for Feb 2014 in Anaheim correspond to one set of sample and sampling was not carried out during Dec 2013 at Anaheim.

a) Central LA

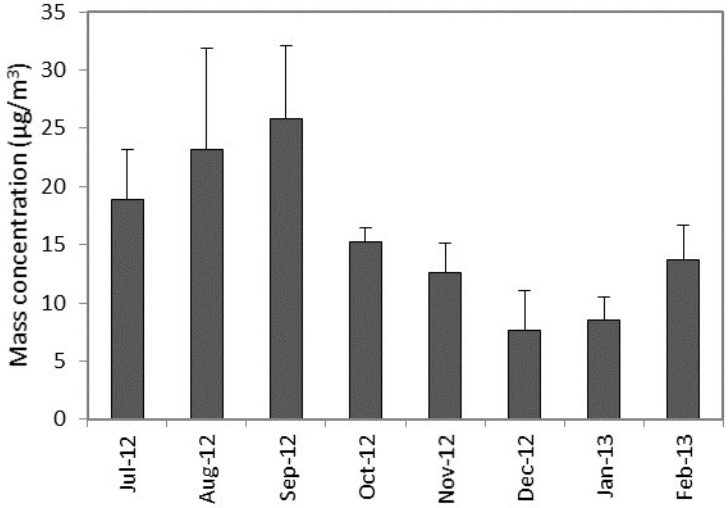

b) Anaheim

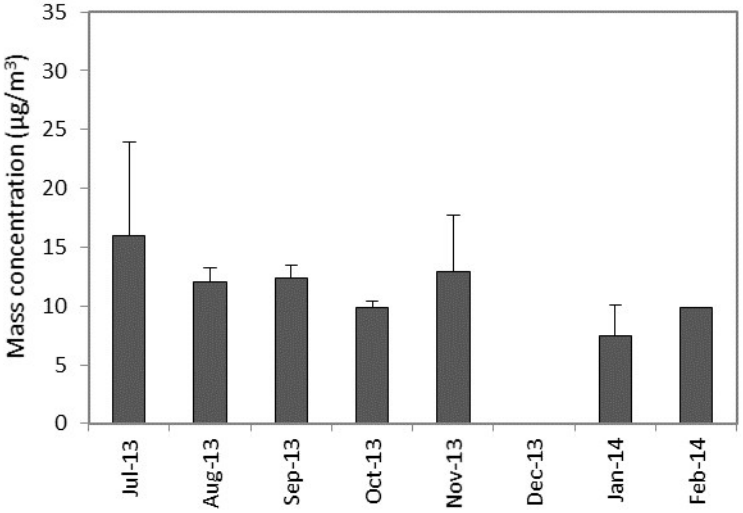

Figure 2 (a-b). Monthly-averaged volume-based water-soluble (WS) and water-insoluble (WI) ROS activity (µg Zymosan/m^3 air) in coarse mode at a) Central LA and b) Anaheim. Sampling was not carried out during Dec 2013 at Anaheim.

a) Central LA

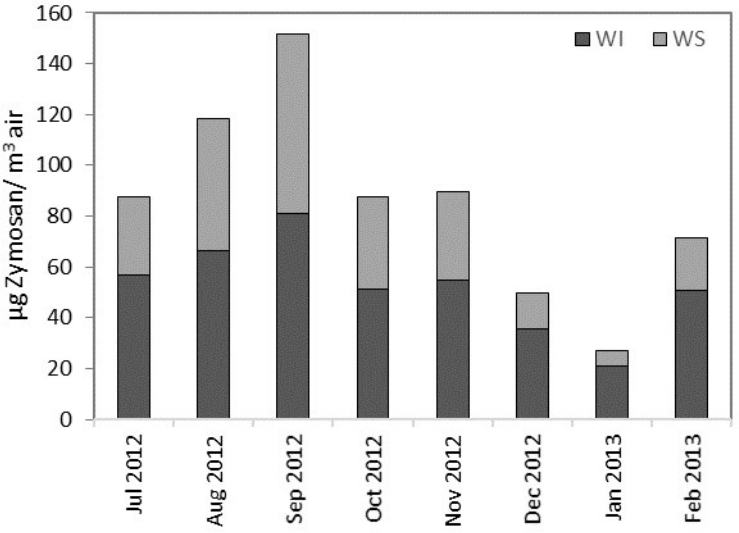

b) Anaheim

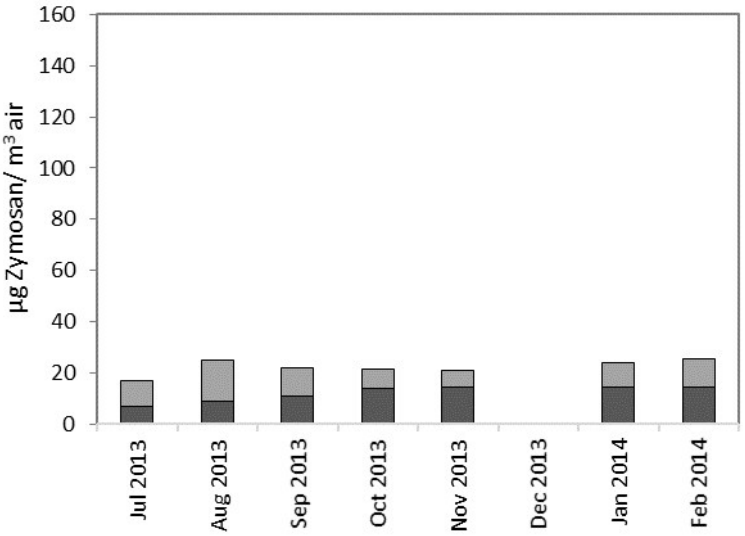

Figure 3 (a-b). Monthly-averaged mass-based water-soluble (WS) and water-insoluble (WI) ROS activity (µg Zymosan/mg PM) in coarse mode at a) Central LA and b) Anaheim. Sampling was not carried out during Dec 2013 at Anaheim.

a) Central LA

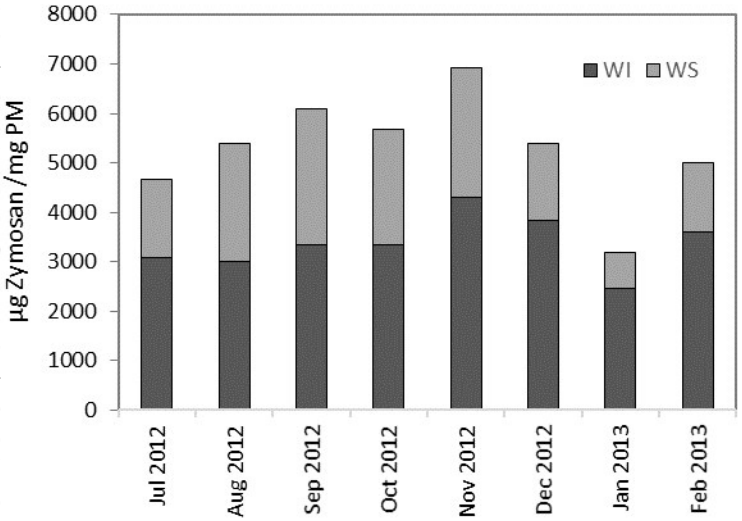

b) Anaheim

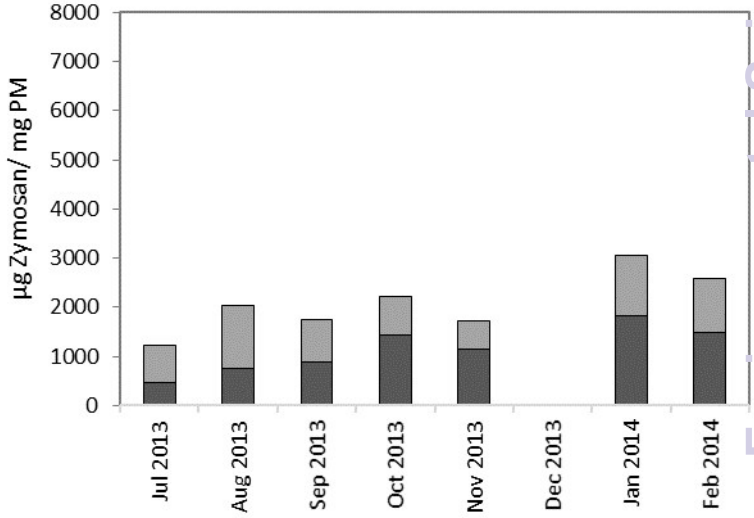

Figure 4 (a-b). Geometric mean concentrations (ng/m^3) of water-soluble (WS) and water-insoluble (WI) metals and elements in coarse mode at a) Central LA and b) Anaheim, over all sampling months. Error bars are standard deviation. Pb was below detection limit in water-soluble fraction.

a)

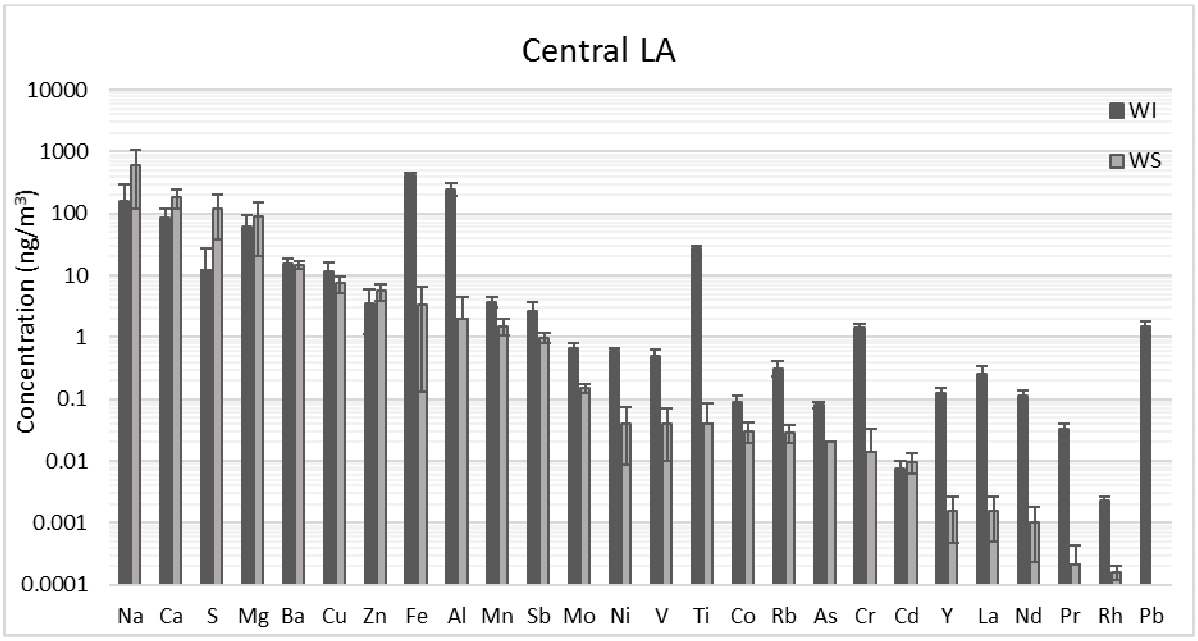

b)

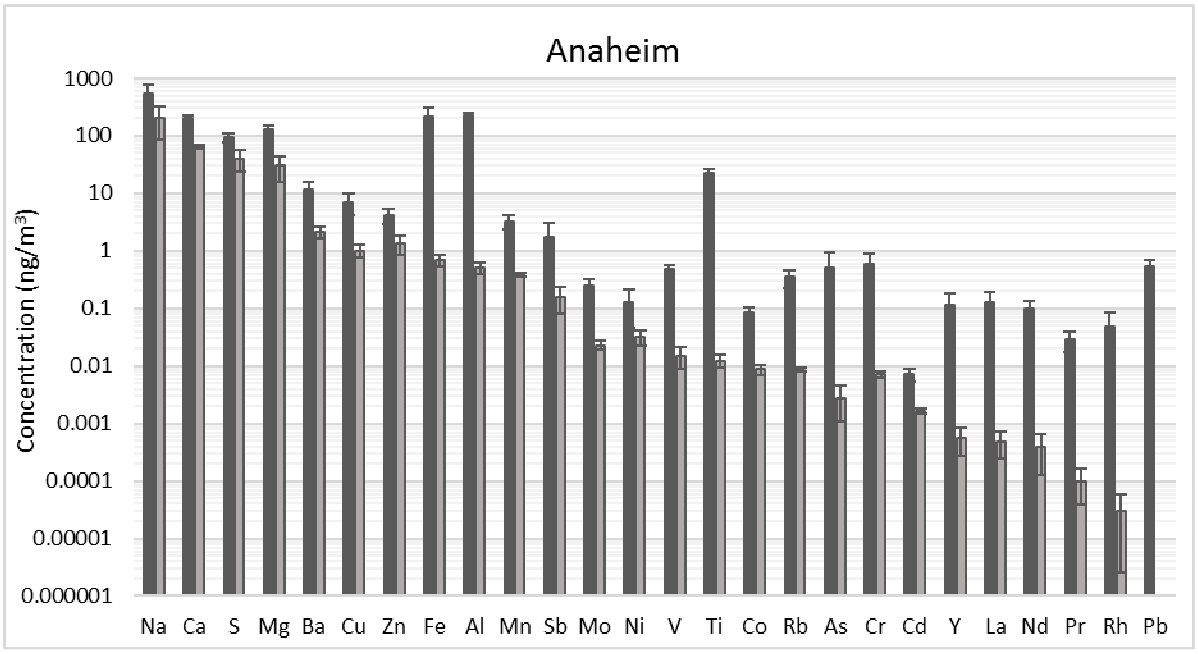

Figure 5 (a-b). Monthly-averaged variation of selected water-soluble metals concentration at a) Central LA and b) Anaheim. Sampling was not conducted on Dec 2013 at Anaheim. Feb 2014 data point corresponds to one sample.

a) Central LA

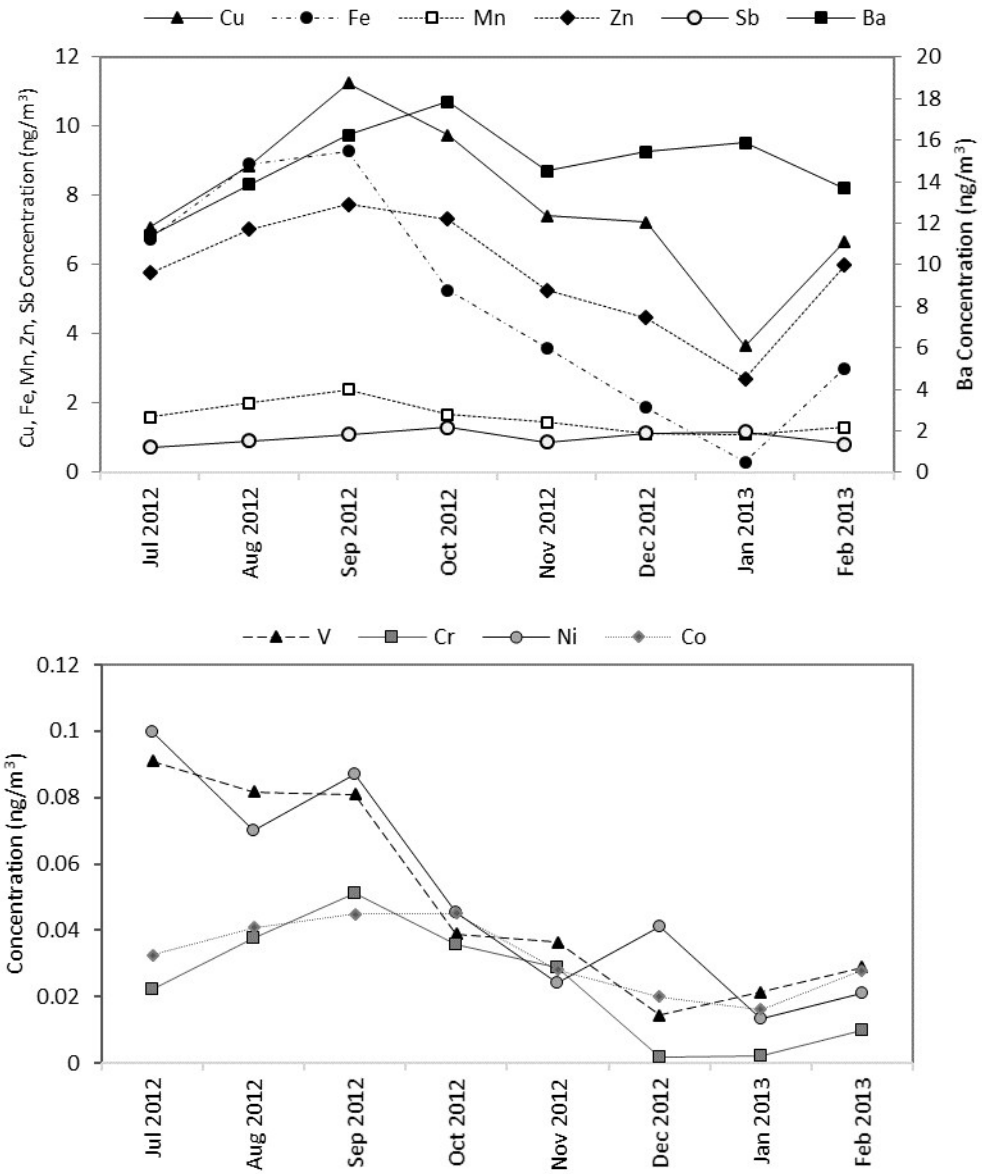

b) Anaheim

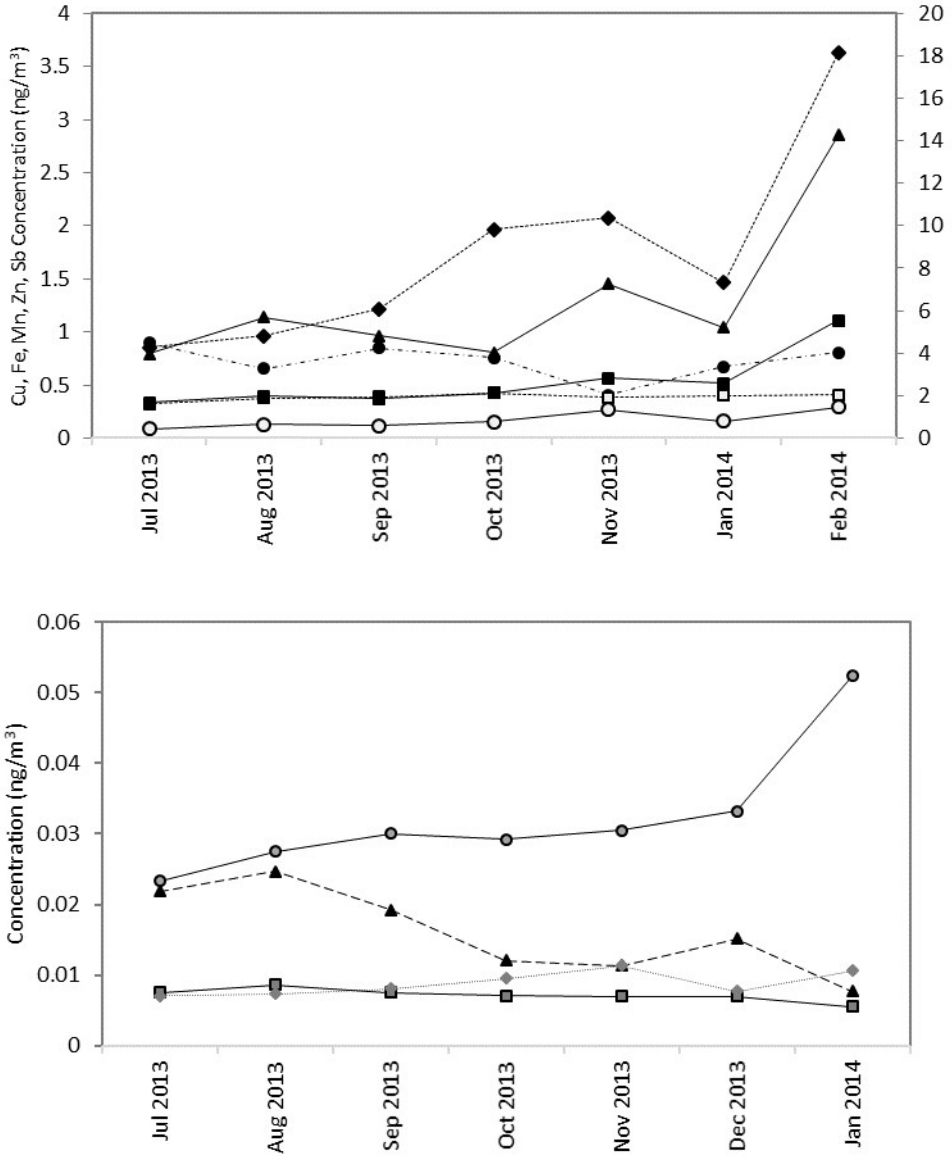

Figure 6 (a-b). Monthly-averaged variation of selected water-insoluble metals concentration at a) Central LA and b) Anaheim. Sampling was not conducted on December 2013 at Anaheim. Feb 2014 data point corresponds to one sample.

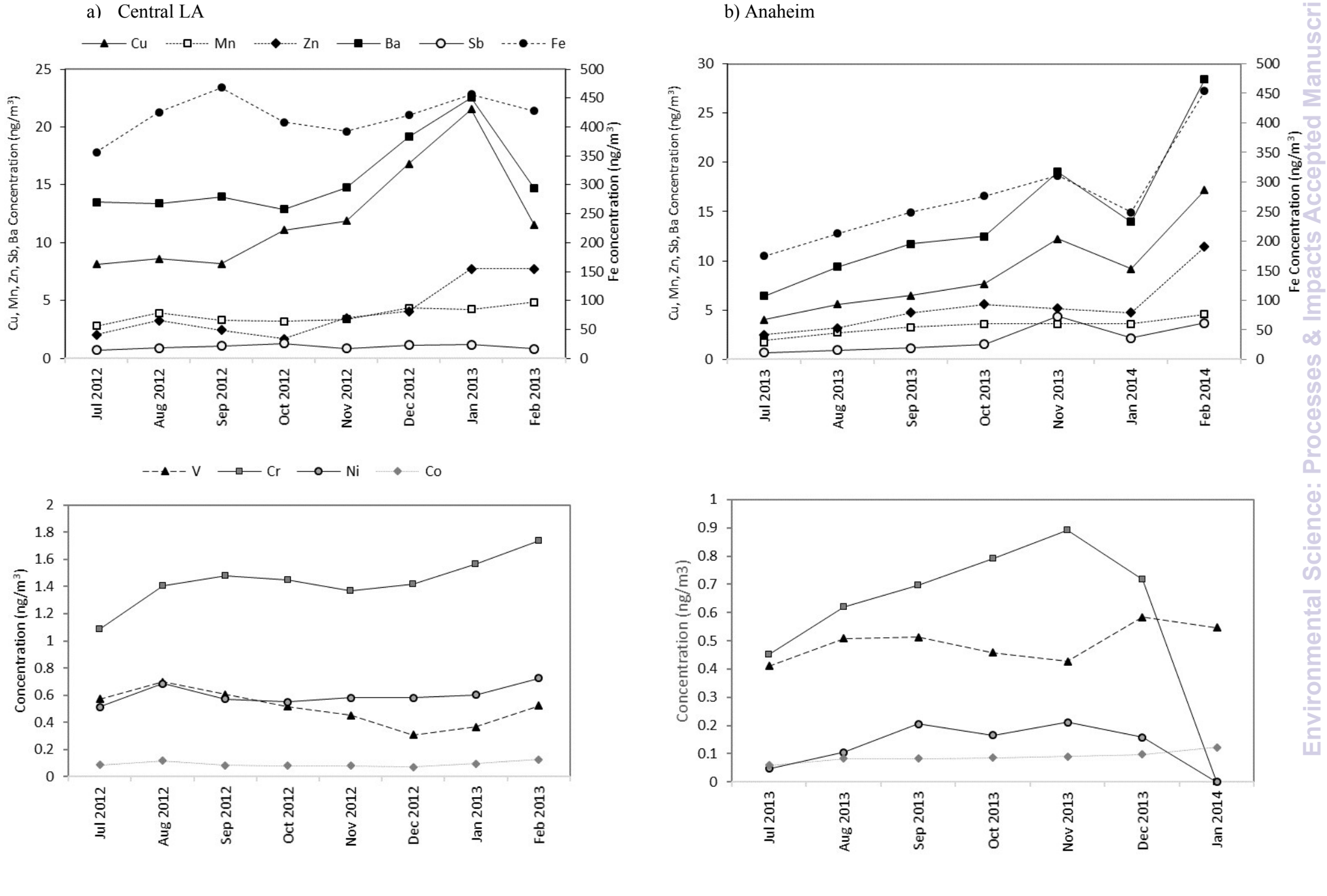

Figure 7 (a-b). Linear regression between measured and modeled volume-based ROS of both sites combined for a) water-soluble, b) water-insoluble fractions.

a)

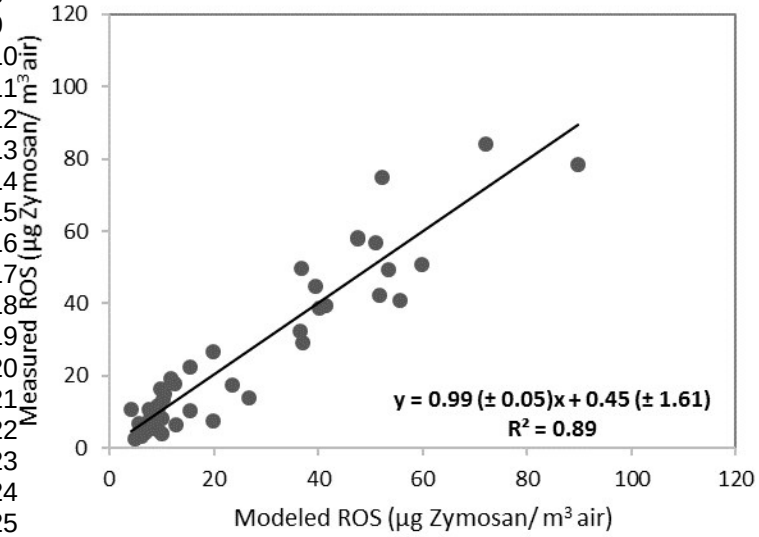

b)

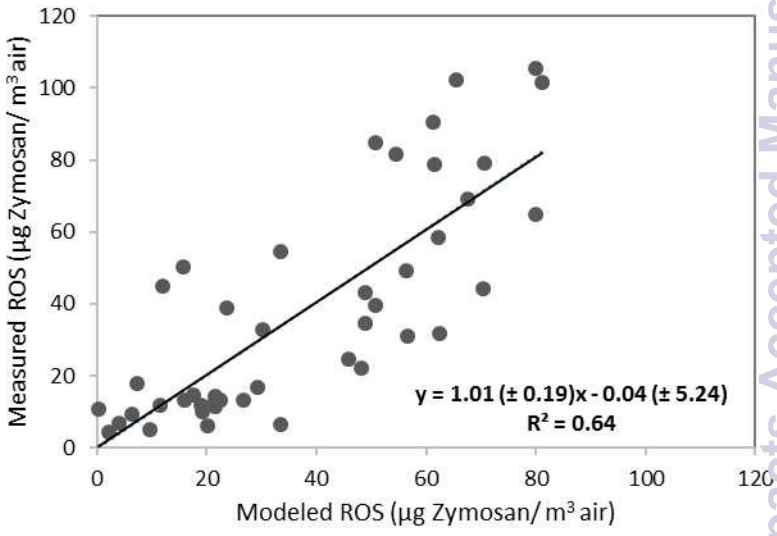

Figure 8 (a-b). Box plots of volume-based ROS activity comparison between Cheung et al., (2012) study and current study at Central LA. Dotted lines represent arithmetic means. The black dots correspond to the 5th and 95th percentiles.

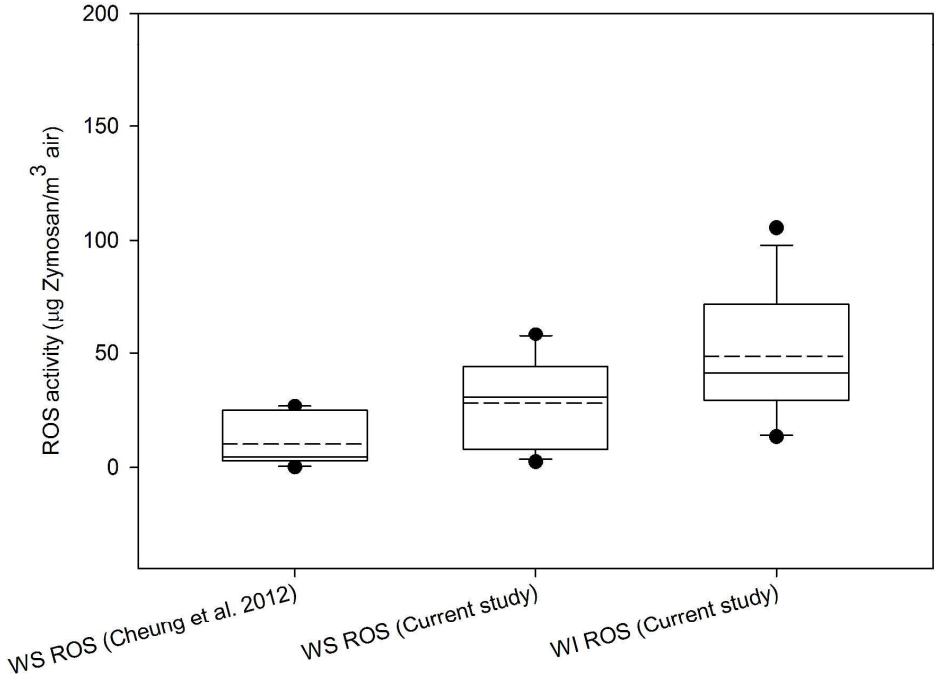

Figure 9. Box plots of groups of metals from Cheung et al., (2012) and current study at Central LA. Dotted lines represent arithmetic means. The black dots correspond to the 5th and 95th percentiles.